



Short communication

A comparison study of capacity degradation mechanism of LiFePO₄-based lithium ion cells

Hui-Fen Jin, Zhen Liu, Yan-Mei Teng*, Jun-kui Gao, Yong Zhao

Tianjin Lishen Battery Joint-Stock Co., Ltd., Tianjin 300384, China

ARTICLE INFO

Article history:

Received 31 July 2008

Received in revised form

26 December 2008

Accepted 31 December 2008

Available online 14 January 2009

Keywords:

LiFePO₄

Lithium ion cell

Capacity degradation

Impurity

Iron deposition

ABSTRACT

The physical properties and electrochemical performance of two kinds of commercialized LiFePO₄ (hereafter abbreviated as LFP) were analyzed. And the cycle stability of the two kinds of material in the 18,650 type lithium ion cells was measured at different charge cut-off voltage (3.65, 3.8, 4.0 and 4.2 V). The two kinds of material showed remarkable difference. One has good cycle stability but another encounters serious failure problem at high charge cut-off voltage (4.2 V). Results showed that the impurities containing iron atom in the raw material and formed during the charge–discharge cycles are the main reasons of the failure mechanism. The impurities were reduced on the graphite surface and iron dendrite formed gradually, which may penetrate through the separator and results in the inner short circuit of the cells.

© 2009 Elsevier B.V. All rights reserved.

1. Introduction

Since LFP with an olivine-type structure was first reported as a positive electrode for lithium ion cells in 1997 by John Goodenough and coworkers, it has showed a great prospect for its outstanding nature. LFP with an olivine-type structure has good stability, high temperature of releasing oxygen, rich resources and environment friendly as compared with traditional cathode material LiCoO₂, LiNiO₂ and LiMn₂O₄ [1–4]. The cells with LFP as cathode material are the ideal batteries for electric tools, electric vehicles and other electric equipments. The researches of LFP mainly focused on the improvement of the ion conductivity, the bulk specific weight and lowering the price [5–8]. Few studies have been made on the stability of LFP in a Li ion cell configuration. Nowadays, many companies declared that they commercialized the LFP, but there are large differences of physical properties and electrochemical performance among the commercialized samples which are different from that of commercialized LiCoO₂. We found that the capacity of some samples degrade dramatically at the charge cut-off voltage of 4.2 V. Interestingly, the degradations did not occur in the former stage of charge–discharge cycles, but occurred after about 200 cycles or even after more than 300 cycles. This failure is very important for the lithium ion cells. In this study, the cycle stability at charge cut-off voltage of 4.2 V of two kinds of commercialized

LFP material were measured, and the failure mechanism was analyzed.

2. Experimental

The two kinds of commercialized LFP material were obtained from Valence (A) and BTR (B). They have similar particle size distribution.

Crystalline phases were identified with X-ray diffraction (XRD, Rigaku D/max-2550). XRD patterns were collected by a step-scanning mode in the range of 10–80° with a step time of 5° min⁻¹.

The morphology of the materials was observed with a scanning electron microscopy (SEM, JEOL JSM-6360). The element analysis on the separator was conducted with an energy-dispersive X-ray spectrometer (EDS, EDAX GENESIS60s).

The contents of Fe³⁺ in the raw materials were measured by colorimetry and iron content in the anode after charge–discharge cycles was analyzed by inductively coupled plasma (ICP, Thermo Electron, IRIS Intrepid || XSP).

The electrodes using raw materials of A and B were prepared with PVDF as binder, carbon black as conductor mixed in a 92:4:4 ratio (wt.%) and aluminum foil as current collector. Before we made the electrode, the raw materials of A and B had been dried by vacuum dry boxes for 4 h in the condition of 130 °C, –100 kPa. Then A or B with PVDF and carbon black mixed round for 12 h, in the solvent of NMP. The amount of NMP was controlled until the viscosity reached 8 Pa S. After mixing, the mixture was coated on the aluminum foil as electrodes, heating in the coating process. Then

* Corresponding author. Tel.: +86 22 83716755; fax: +86 22 83716859.

E-mail address: ct062085@lishen.com.cn (Y.-M. Teng).

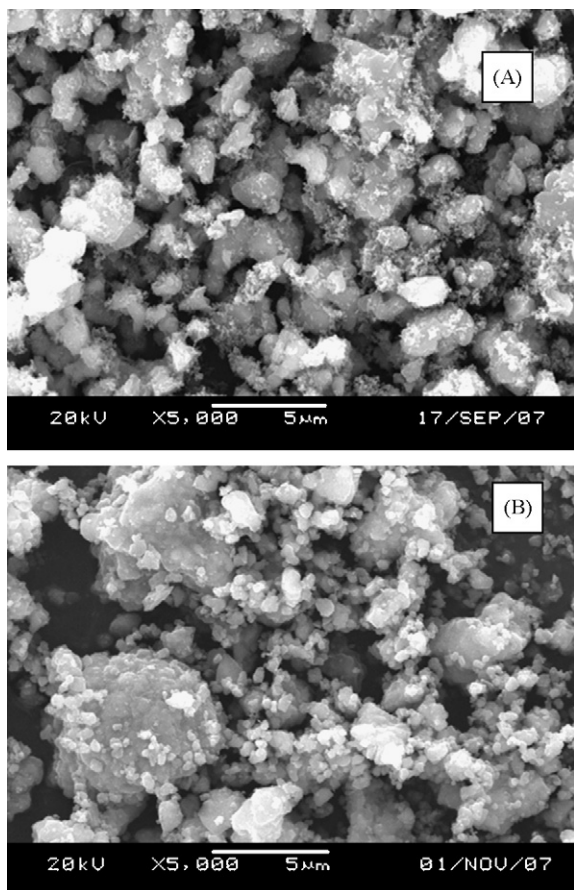


Fig. 1. The SEM of raw samples A and B.

the electrodes were calendered. The electrodes had the same coating density and electrode density. After the electrodes were made, they were dried by vacuum dry boxes for 12 h in the condition of 110 °C, –100 kPa. The prepared process of negative electrodes was the same. The negative electrodes were prepared with graphite as active material, PVDF as binder, carbon black as conductor mixed in a 90:6:4 ratio (wt.%) and copper foil as current collector. The electrode after drying was assembled in an 18,650 type case with 1.0 mol L⁻¹ LiPF₆ in EC + DEC + EMC with 1:1:1 volume ratio as elec-

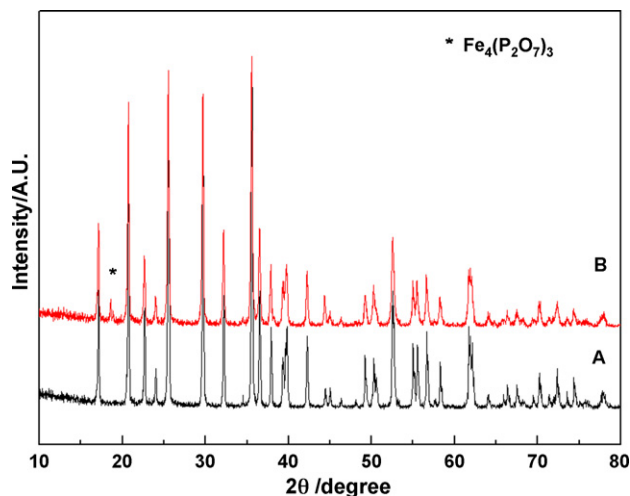


Fig. 2. XRD pattern of raw samples A and B.

trolyte. The separator was Celgard2320. All the assembly process was done in the dry-room.

The nominal capacity is 1300 mAh and were tested with 1C rate by Arbin (BT2000) with the following program: the cells were charged to 3.65, 3.8, 4.0 and 4.2 V with 1C rate, respectively, then charged with constant voltage until the current decreased to 0.02C, then discharged to 2.0 V with 1C rate.

The floating charge is as follows: the cells were charged to 3.65, 3.8, 4.0 and 4.2 V with 1C rate, respectively, and then charged with constant voltage for 1-week.

3. Results and discussion

3.1. Physical properties

The SEM of the two kinds of samples was shown in Fig. 1. It shows that the particle size of sample A is smaller than that of B and the particle size distribution is more homogeneous than that of B. There are large particle (>5 µm) distributed in the sample. Samples A and B are prepared by solid reaction and coated with the same content of carbon (4%). The carbon coating improves the electron conductivity, which is considered as the main barrier for the commercialized of LFP.



Fig. 3. The standard solution (left) with nine contents of Fe³⁺: 0.2, 0.3, 0.5, 0.8, 1.0, 1.5, 2.0, 2.5 and 3.0 wt.%; Tested samples A and B solution (right).

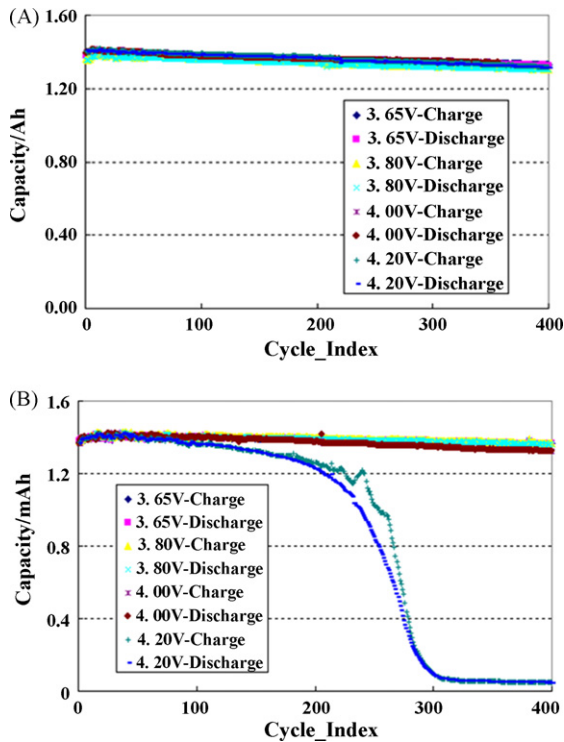


Fig. 4. The charge and discharge capacities change with cycle number.

Fig. 2 shows the XRD pattern of the samples A and B. The peaks of the powder A are corresponding to an olivine orthorhombic structure type (space group: Pnma), whereas the pattern of powder B shows a second phase $\text{Fe}_4(\text{P}_2\text{O}_7)_3$ exists as asterisk indicated.

The contents of Fe^{3+} of the powder A and B were measured by colorimetry. A series of standard solutions with different content of Fe^{3+} : 0.2, 0.3, 0.5, 0.8, 1.0, 1.5, 2.0, 2.5 and 3.0 wt.% was compared with the sample solution. The results demonstrated that the content of Fe^{3+} of powder B is about 10 times higher than that of powder A, which was shown in Fig. 3.

3.2. Electrochemical performance

The charge and discharge capacities change with cycle number are shown in Fig. 4. The charge cut-off voltage of the two cells is 4.2 V. Results showed that cells with material A as cathode showed a continuous capacity degradation but cells with material B as cathode showed a dramatic degradation after 200 cycles, furthermore, the charge capacities of cells with B as cathode were larger than discharge capacities at the following cycles and the capacity decreased to about 0 after 300 cycles. The AC resistance of the two cells was measured and results showed that the AC resistance of cells with sample B as cathode increased 221% but that of sample A as cathode only increased 43%.

3.3. Failure mechanism analysis

Fig. 5 shows the XRD patterns of the cathodes separated from cells with A and B after 400 cycles. For the sample A, no other diffraction peaks except LiFePO_4 are observed. But for the sample B, a diffraction peak at 2θ 26.52° as plus sign indicated can not be identified, and the other peak at 2θ 18.58° as asterisk indicated attributes to $\text{Fe}_4(\text{P}_2\text{O}_7)_3$.

The cells with sample B as cathode were disassembled to analyze the reason for capacity degradation. Many black dots appeared on the separator, which were shown in Fig. 6(a). The distribution of

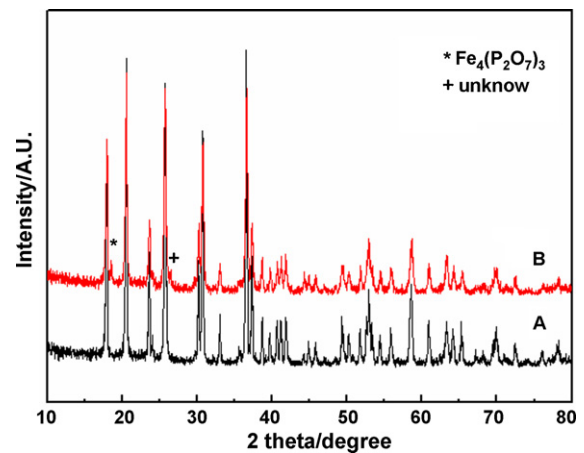


Fig. 5. XRD of samples A and B got from electrode after cycled.

the black dots on separator is random. EDS (Fig. 6(b)) results that the black dots are metal iron. Metal iron may form Fe dendrite and penetrate through the separator and result in micro short circuit of the cells.

Fig. 7 showed the Fe contents in the anode electrode separated from cells with A and B as cathode, respectively, which was

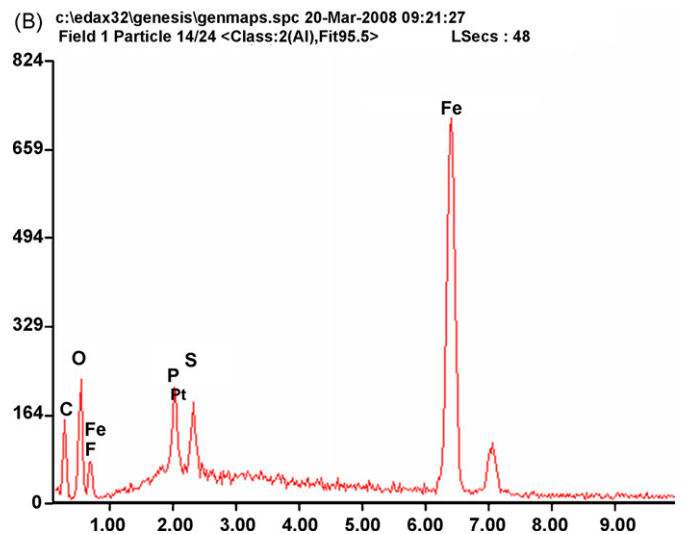


Fig. 6. (a) The photo of the black dots on the separator after charge–discharge cycle of B. (b) The EDS of the black dots on the separator after charge–discharge cycle of B, all the letters on the graph are elements of the black dots, such as C, O, F, P, S and Pt.

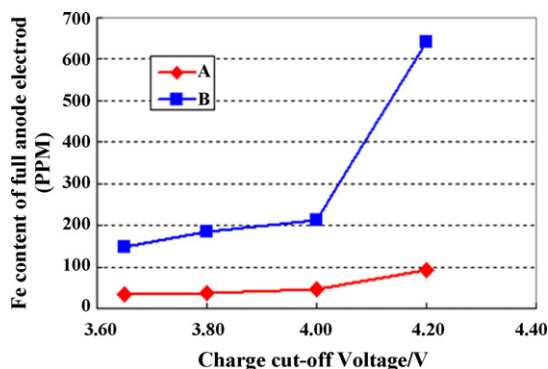


Fig. 7. The iron contents in the anode electrode of the cells prepared with samples A and B after 400 charge–discharge cycles.

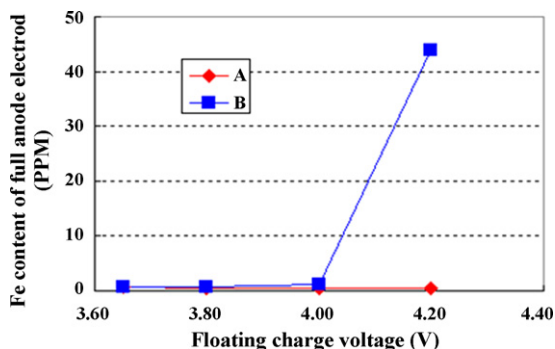


Fig. 8. The iron contents in the anode electrode of the cells prepared with samples A and B as cathode after floating charge for 1-week.

charged–discharged for 400 cycles with different charge cut-off voltage and the full anode electrode was measured by ICP. The iron contents in the anode of cells with B as cathode increased slowly as the charge cut-off voltage increased to 4.0 V, but increased sharply to 650 ppm when the charge cut-off voltage increased to 4.2 V. However, the iron contents in the anode of cells with sample A as cathode remain at the same level with charge cut-off voltage

increased to 4.0 V, and that increased to less than 100 ppm at the charge cut-off voltage of 4.2 V. The results of ICP measurement are in good correspondence with the cycle performances of these cells. Floating charge tests at different voltage were conducted to further confirm the relation between iron content in the anode and capacity degradation. Fig. 8 shows the iron contents measured by ICP in anodes separated from cells with samples A and B as cathode after floating charge at different voltage for 1-week. Similar results are obtained from the curves. The iron contents in the anodes electrode of cells with A as cathode had little change in the floating charge voltage range of 3.65–4.2 V, whereas that of cells with B as cathode increased dramatically at the floating charge voltage of 4.2 V. The results indicate that metal iron deposited on the anode is the major reason for the capacity degradation at high charge cut-off voltage, and the metal iron contents deposited on anode have close relation with the Fe^{3+} contents of the fresh powder, i.e. the impurities.

4. Conclusions

In this paper, capacity degradation mechanism of two kinds of LiFePO_4 materials at high charge cut-off voltage was studied. Results showed that the impurities containing iron atom in the raw material and formed during the charge–discharge cycles are the main reasons of the failure mechanism for the cells with material B as cathode. The impurities were reduced on the graphite surface and dendrite formed gradually, which may penetrate through the separator and resulted in the inner short circuit and the failure of the cell.

LFP material producing process must be controlled more strictly.

References

- [1] A.K. Padhi, K.S. Nanjundaswamy, J.B. Goodenough, *J. Electrochem. Soc.* 144 (1997) 1188.
- [2] A.S. Andersson, J.O. Thomas, *J. Power Sources* 97–98 (2001) 498.
- [3] S.Y. Chung, J.T. Bloking, Y.-M. Chiang, *Nat. Mater.* 1 (2002) 123.
- [4] J. Chen, M.S. Whittingham, *Electrochem. Commun.* 8 (2006) 855.
- [5] A. Yamada, S.C. Chung, K. Hinokuma, *J. Electrochem. Soc.* 148 (2001) A224.
- [6] M. Takahashi, S. Tobishima, K. Takei, Y. Sakurai, *J. Power Sources* 97–98 (2001) 508.
- [7] K. Amine, J. Liu, I. Belharouak, *Electrochem. Commun.* 7 (2005) 669.
- [8] H.H. Chang, C.C. Chang, H.C. Wu, *Electrochem. Commun.* 10 (2008) 335.